Infrasound: Connecting the Solid Earth, Oceans, and Atmosphere

M.A.H. Hedlin,[1] K. Walker,[1] D.P. Drob,[2] and C.D. de Groot-Hedlin[1]

[1]Laboratory for Atmospheric Acoustics, Institute of Geophysics and Planetary Physics, Scripps Institution of Oceanography, University of California, San Diego, La Jolla, California 92093-0225; email: hedlin@ucsd.edu, kwalker@ucsd.edu, chedlin@ucsd.edu

[2]Upper Atmospheric Modeling Section, Naval Research Laboratory, Washington, D.C. 20375; email: douglas.drob@nrl.navy.mil

Annu. Rev. Earth Planet. Sci. 2012. 40:327–54

First published online as a Review in Advance on February 9, 2012

The *Annual Review of Earth and Planetary Sciences* is online at earth.annualreviews.org

This article's doi:
10.1146/annurev-earth-042711-105508

0084-6597/12/0530-0327$20.00

Keywords

gravity waves, ducting, wind noise, coupling, attenuation, scattering

Abstract

The recently reinvigorated field of infrasonics is poised to provide insight into atmospheric structure and the physics of large atmospheric phenomena, just as seismology has shed considerable light on the workings and structure of Earth's solid interior. Although a natural tool to monitor the atmosphere and shallow Earth for nuclear explosions, it is becoming increasingly apparent that infrasound also provides another means to monitor a suite of natural hazards. The frequent observation of geophysical sources—such as the unsteady sea surface, volcanoes, and earthquakes—that radiate energy both up into the atmosphere and down into the liquid or solid Earth and transmission of energy across Earth's boundaries reminds us that Earth is an interconnected system. This review details the rich history of the unheard sound in the atmosphere and the role that infrasonics plays in helping us understand the Earth system.

1. INTRODUCTION

For decades, researchers have studied the physics of our planet using an extraordinarily broad suite of instruments deployed in every environment from deep within Earth to outer space. Of Earth's environments, the atmosphere is the most dynamic. What happens in our atmosphere, or what is going to happen in the near future, is critically important to us, whether we are interested in the development of a major storm crossing the Atlantic or the winds and turbulence an airplane is likely to encounter in flight. Although a broad suite of instruments has been used to probe the atmosphere, one area of research that has lagged is the acoustics of the atmosphere—specifically, long-period acoustics. This seems surprising, as infrasonics is a close cousin of seismology, which is the key technology for studying Earth's interior, its structure, and the sources active within it. Infrasonics is applied to the atmosphere with similar objectives but on a much smaller scale.

We begin this review with a brief description of infrasonics before discussing its reemergence as a field of active study during the past decade; the promise of infrasonics in providing another means to probe Earth's atmosphere; and its promise in providing another means to remotely uncover the physics of significant geophysical phenomena active in the atmosphere, at Earth's surface, or within Earth's shallow crust. Infrasonics is a new means to monitor a broad range of natural hazards. It is one of the primary tools the international community uses to monitor for nuclear explosions. It is this practical application that has served as an impetus for the basic research that much of this review describes. We also explain the complexities involved in monitoring infrasound. Specifically, we discuss the constantly varying atmosphere, wind noise at recording sites, and the paucity of infrasonic recording stations. Lastly, we review the hypotheses for how certain natural sources generate infrasound.

2. INFRASOUND AND THE ACOUSTIC SPECTRUM

Although we are all familiar with many of the sounds that surround us, there is a continuous unheard panoply of sounds outside the frequency range of human hearing. The nominal range of human hearing is 20–20,000 Hz; ultrasound is at frequencies above the audible range, and infrasound is at frequencies below the audible range. Infrasound relates to audible sound as infrared electromagnetic energy relates to visible light. Like infrared signals, these infrasonic signals can be observed only on instruments or through the effect on surrounding structures (for example, vibrations of windows). A wide variety of atmospheric phenomena compress enough air to produce sounds in Earth's atmosphere at infrasonic frequencies. Below the deepest range of infrasound—acoustic waves with periods of approximately 60 s, corresponding to wavelengths that are greater than ~20 km—buoyancy forces are important, and gravity becomes an important factor governing propagation. Acoustic-gravity waves are generated by large-scale atmospheric phenomena. These long-period waves are valued for research because they attenuate slowly and can be detected at ranges of hundreds to thousands of kilometers.

3. OUR EARLY EXPERIENCES WITH INFRASOUND

A thorough review of the history of infrasonics can be found in numerous papers (including Evers & Haak 2010). Only a brief account is given here. The cataclysmic eruption of Krakatoa in 1883 is often cited as the event that gave rise to the science of infrasonics and to studies of atmospheric structure. Reports of cannon fire on August 27 and 28 of that year reached the Royal Society office in London, followed by a stream of ~50 barometric recordings from around the world (Symons 1888). All were eventually attributed to the eruption of Krakatoa, still considered the loudest

sound in recorded human history. The instruments registered a sequence of arrivals spanning several days. These wave trains were interpreted as acoustic-gravity waves from Krakatoa, some of which circled the globe several times. The recordings were used in a scientific study of the speed of sound (Symons 1888). In the decades that followed the Krakatoa eruption, occasional, singular events (including the Tunguska event above Siberia and the Baden Aniline and Soda Factory plant explosion in Germany in 1921) briefly attracted interest in infrasound and gravity waves. Although infrasound was routinely monitored during World War I to locate enemy aircraft, the field remained little more than an occasional scientific curiosity until the nuclear age began with the Trinity test in New Mexico in 1945, which showed that infrasound had clear value in detecting and locating atmospheric nuclear tests. After the Trinity test, infrasonics was finally pursued as a science, and research proceeded on numerous fronts including noise reduction, sensor design, array design, propagation, and source physics. Perhaps the key advance during this era was the development by Fred Daniels of spatial filters to reduce noise from wind flow near the sensor.

Although interest in infrasound waned with the Limited Test Ban Treaty, which banned atmospheric nuclear tests, interest was rekindled when many world nations signed the recent Comprehensive Nuclear Test Ban Treaty, which called for monitoring of the entire globe, including the atmosphere. This treaty came with four monitoring networks, including a 60-station network of 1–3-km aperture infrasonic arrays (**Figure 1**) capable of locating a 1-kiloton nuclear explosion in the atmosphere. Although infrasound has been used for practical purposes (for instance, detecting and locating aircraft; detecting, locating, and identifying nuclear-explosion tests; and monitoring volcanoes, avalanches, and major storms), it has also been applied to basic research (for instance, to expand our understanding of geophysical phenomena in the atmosphere or at Earth's surface and

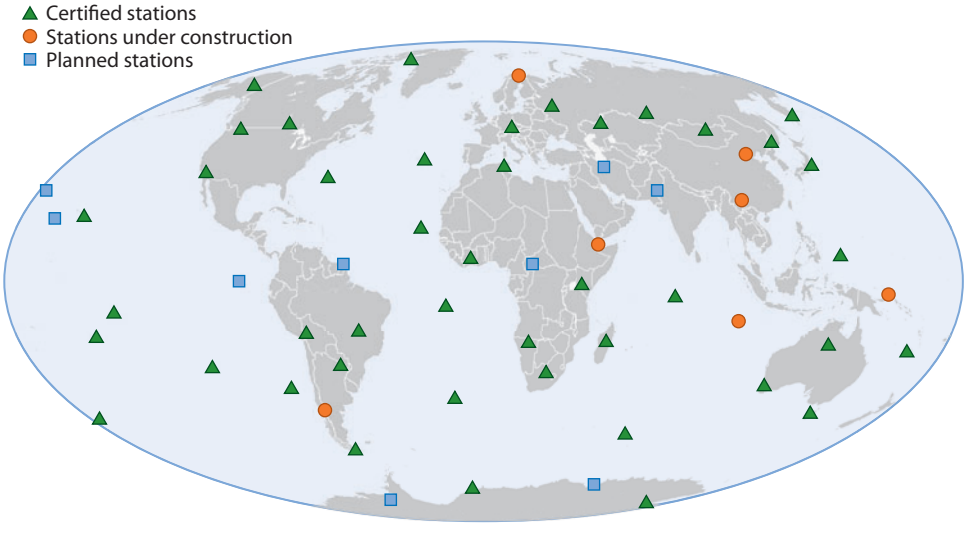

Figure 1

The infrasonic array network, a component of the Comprehensive Nuclear Test Ban Treaty Organization's International Monitoring System. Green triangles represent certified stations that transmit data in near real time to the International Data Center in Vienna, Austria. Orange circles and blue squares represent stations under construction or still in the planning stage (as of June 4, 2011). Each completed station is an array comprising several microbarometers spanning an area 1–3 km across. Each sensor is equipped with a spatial noise filter. Upon their completion, the average distance between adjacent stations will be ~2,200 km.

as an atmospheric probe, particularly at altitudes not well constrained by ground- or space-based instruments).

4. ATMOSPHERIC STRUCTURE AND INFRASONIC PROPAGATION

Infrasonic propagation is controlled by a variety of phenomena: advection through a windy atmosphere, refraction due to sound speed gradients, reflections by ground topography, attenuation due to the absorptive properties of the upper atmosphere, and scattering and diffraction at small-scale atmospheric perturbations due to turbulence or gravity waves. In the near field, infrasonic signals are attributable to direct line-of-sight arrivals from the source. At greater distances, vertical gradients in the wind speed profile and sound speed profile can result in the ducting, or channeling, of infrasound between the ground and the lower, middle, or upper atmosphere, allowing the energy to propagate to ranges of thousands of kilometers.

Infrasonic ducts vary both spatially and temporally. For this reason, sources may generate infrasonic signals that are detected at one location but not at another nearby location (e.g., de Groot-Hedlin et al. 2008, Hedlin et al. 2010). Infrasonic detection also depends on the season (Le Pichon et al. 2002, Arrowsmith & Hedlin 2005) or the time of day because of changes in atmospheric conditions (Fee & Garcés 2007). Historically, similar variations in audible sound recordings led to further insight into atmospheric conditions at altitudes of 10–50 km (Whipple 1935, Gutenberg 1939). More recently, infrasonic detections have been used to infer properties of winds at even greater altitudes (e.g., Le Pichon et al. 2005). Here, we provide a brief description of spatiotemporal variations in atmospheric conditions relevant to the ducting of infrasound; a much more detailed explanation is provided in de Groot-Hedlin et al. (2010).

Tropospheric, i.e., lower atmospheric, ducts are a transient, primarily diurnally varying phenomenon. Usually air temperatures are highest near the ground owing to the absorption of solar radiation at Earth's surface, and they drop with altitude owing to the decrease in atmospheric density. The average lapse rate of 6 K km^{-1} corresponds to a decrease in sound speed of nearly 4 m s^{-1} per kilometer of altitude through the relation $c = 20.05T^{1/2}$ m s^{-1}, where T is the temperature in degrees Kelvin (K). The typical decrease in sound speed with altitude causes infrasound to refract upward away from Earth's surface. However, cooling air temperatures near ground level at night and early in the day can combine with the tropospheric jet stream to give rise to short-lived tropospheric ducts.

The stratosphere, just above the troposphere, extends from an altitude of approximately 10–20 km to 50 km, depending on the latitude. Stratospheric ducting of infrasound between the ground and the stratopause results from the effects of a rise in temperature with altitude within the stratosphere combined with the effects of seasonal variations in zonal (east–west) stratospheric winds (**Figure 2**). The temperature increase is due to the interaction between solar ultraviolet radiation and ozone within the stratosphere, but this rise is rarely sufficient to cause ducting without the addition of the zonal winds. In the Northern Hemisphere, stratospheric winds flow westward in summer and eastward in winter, enhancing ducting along the wind-bearing direction and diminishing it along the opposite direction. Thus, in the Northern Hemisphere, infrasonic observations are enhanced to the west of a source in summer and to the east in winter (as shown in **Figure 2**). Spring and autumn are transitional periods during which stratospheric arrivals may be completely absent.

Atmospheric temperatures decrease rapidly in the mesosphere—which extends from approximately 50 km to 90 km—owing to greater infrared cooling by carbon dioxide. Temperatures increase sharply in the thermosphere—at altitudes over 90 km—owing to absorption of extreme ultraviolet radiation by small amounts of oxygen present. Regardless of wind speed in the

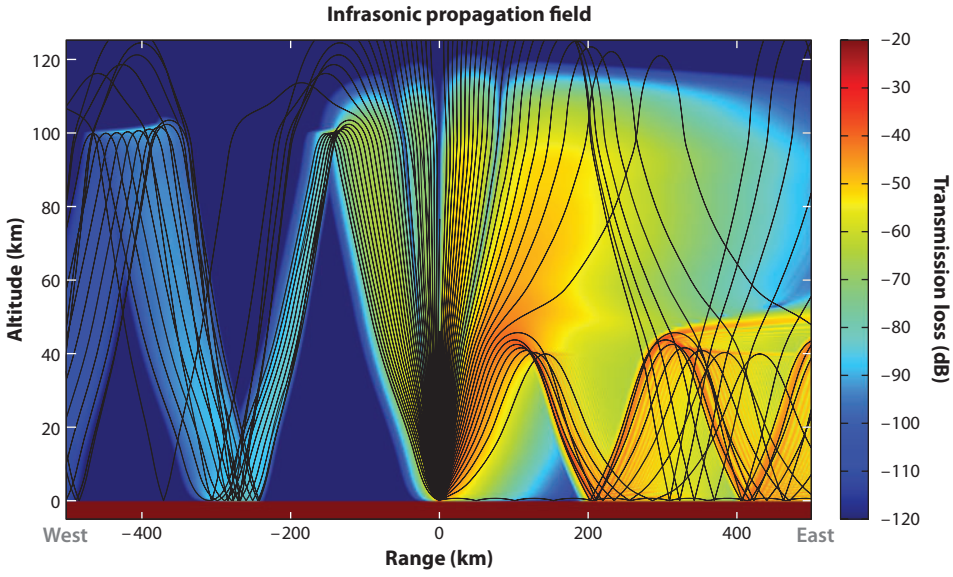

Figure 2

The typical anisotropic nature of infrasonic ducting for a typical boreal winter. Stratospheric ducting near 40-km altitude occurs with eastward propagation with the direction of the stratospheric jet, and thermospheric ducting also occurs in this direction. Only thermospheric ducting occurs for westward propagation. This profile illustrates geometric shadow zones (regions of low sound pressure from the source) within 200 km of the event in both directions.

thermosphere, the increased air temperature is sufficient to cause thermospheric ducting. Nevertheless, thermospheric returns are rarely observed for frequencies above ~1 Hz, presumably owing to anticipated extreme acoustic absorption within the upper atmosphere. Acoustic absorption mechanisms can be categorized in terms of classical losses (which are due to viscosity, heat conduction, and diffusion) and molecular vibration losses (which involve the excitation of the energy of the gas molecules in the atmosphere) (e.g., Ejakov et al. 2003). At infrasonic frequencies, molecular relaxation is dominant at altitudes below ~60 km, and the associated attenuation increases with the square of the frequency (Pierce 1989). Classical losses, which increase with the square of the frequency and the reciprocal of the density (Pierce 1989), dominate at higher altitudes. Thus, for purely linear propagation, only extremely low-frequency thermospheric returns are predicted, owing to high acoustic absorption with increasing frequency within the thin upper atmosphere.

The atmosphere varies widely from its global average state as a function of latitude, longitude, season, and time of day. In addition, internal atmospheric buoyancy waves (commonly known as gravity waves, as opposed to gravitational waves) with periods from 6 h to ~1 min and wavelengths from 10 km to 2,000 km are prevalent in the atmosphere. The effects of the various scales of atmospheric variability on infrasonic propagation are discussed in detail below.

5. SYNERGY WITH SEISMOLOGY

Much of Earth's geophysical activity occurs at or near its free surface. Many of these sources (e.g., volcanic eruptions, shallow earthquakes) radiate energy both down into the solid Earth and up into the atmosphere. Some studies (e.g., Matoza et al. 2007) have illustrated how a more complete source model can be obtained from a joint analysis of seismic and infrasonic recordings

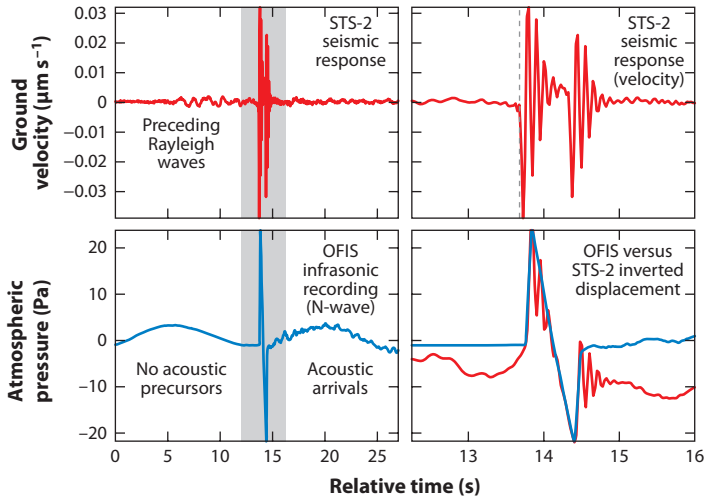

Figure 3

Comparison between the seismic (*top*) and infrasonic (*bottom*) recordings for USArray Transportable Array station 109C (located at Camp Elliott near San Diego, California). The gray bars in the left-hand panels indicate the time intervals displayed in the right-hand panels. The vertical dashed gray line marks the picked arrival times based on the seismic data. The integral of the seismic velocity record is plotted (*red line*) with the infrasonic recording in the lower-right panel. Abbreviation: OFIS, Optical Fiber Infrasound Sensor; STS-2, Streckheisen broadband seismometer. Redrawn with permission from de Groot-Hedlin et al. 2008 [de Groot-Hedlin CD, Hedlin MAH, Walker K, Drob D, Zumberge M. 2008. Study of propagation from the shuttle Atlantis using a large seismic network. *J. Acoust. Soc. Am.* 124(3):1442–51]. Copyright 2008, Acoustic Society of America.

of seismoacoustic sources. There is a natural synergy between seismology and infrasonics not only because they share a link to some sources but also because Earth's free surface is not an opaque boundary to either seismic or infrasonic energy (e.g., Arrowsmith et al. 2010). It is well known that infrasound impinging on the free surface from above readily couples to seismic waves in the solid Earth that can be observed in seismic records (e.g., Kanamori et al. 1991, Langston 2004, de Groot-Hedlin et al. 2008, Arrowsmith et al. 2010). Likewise, numerous studies have examined or exploited the conversion of seismic energy to infrasound (e.g., Le Pichon et al. 2003, 2006b). For example, **Figure 3** shows an N-wave generated by the shuttle Atlantis as it passed at Mach 5 approximately 35 km above a broadband seismometer and a colocated infrasonic sensor in southern California.

6. THE PROMISE OF INFRASONICS

A distinctly new type of data collected on a large scale should lead to significant advances in the data's associated field as it either offers new constraints on geophysical phenomena as a stand-alone technology or provides information missed by other technologies. As mentioned above, there is a significant link between infrasonics and seismology owing to sources that emit both types of energy and owing to coupling between the two at Earth's free surface. A broad range of phenomena emits infrasonic signals. Many natural sources (such as the unsteady sea surface, bolides, earthquakes, large avalanches, and large storms) in addition to human-made sources (such as nuclear and chemical explosions, rocket launches, supersonic aircraft) generate infrasound (Le Pichon et al. 2002, Bass et al. 2006). With the growing network of infrasonic arrays, this technology is now

being used to probe basic source physics, to provide new constraints on atmospheric structure (e.g., Garcés 2004, Le Pichon et al. 2005, Drob et al. 2010b), and to monitor for nuclear explosions and natural hazards. Infrasonic instrumentation is in increasing use alongside seismic instrumentation in monitoring volcanoes for hazardous releases of ash (Garcés et al. 2008).

7. CHALLENGES FACING THIS FIELD

There are many exciting challenges and opportunities in the field of infrasonics. The research problems being addressed today are perhaps similar in importance to the basic issues seismologists faced in the years when seismic data were first collected on a large scale. Three principal issues in infrasonics are the variable state of the atmosphere, wind noise, and the sparse infrasonic recording infrastructure.

7.1. Atmospheric Variability

Although Earth's interior changes infrequently, at least on human timescales, the atmosphere is in a state of constant flux. For infrasonic propagation purposes, the dynamics of the atmosphere can be described by considering the largest spatiotemporal scales (the seasonal variations) to the smallest (the atmosphere's internal gravity wave spectrum). In between are the weather systems or waves described by synoptic-scale meteorology. Just below these scales, mesoscale phenomenology such as maritime temperature inversion layers, land-sea breeze, nocturnal temperature inversions, and drainage winds also become important. In the middle and upper atmosphere, vertically propagating migrating and nonmigrating tides, driven by the diurnal solar heating of water vapor and ozone in the lower atmosphere, are a dominant part of the spatiotemporal variability of the atmosphere. At the smallest scales throughout the atmosphere, but with increasing importance at higher altitudes, are internal gravity waves.

Pioneering work by Georges & Beasley (1977) and others, which relied on limited knowledge of the atmosphere above 35 km, developed an appreciation for how infrasonic ducting characteristics, primarily stratospheric ducting, vary with latitude over the year. Recently this phenomenology was definitively described by Le Pichon et al. (2009), who summarized the annual variations of four-year cumulative distributions of the infrasonic array detections at acoustic frequencies lower than 2 Hz. The average number of detections as a function of the day-of-year from 36 International Monitoring System (IMS) stations was sorted by increasing latitude and compared with climatological stratospheric wind variations. Clear seasonal zonal wind reversals in the stratosphere along with clear seasonal variations of infrasonic back azimuths were observed. In the Northern Hemisphere and during summer (from June to August), signals from easterly directions dominate; during winter (from November to January), signals from westerly directions dominate. However, the work of Le Pichon et al. (2002, 2005) states that for any specific station and source location (e.g., volcanic eruptions), there are hourly, daily, and seasonal changes of the observed infrasonic propagation characteristics. The latter work focuses on utilizing the observed differences between observed and calculated infrasonic characteristics to revise atmospheric specifications and perform atmospheric acoustic tomography.

Propagation modeling efforts to describe these observed variations, such as those by Drob et al. (2003), utilized observationally based ground-to-space (G2S) atmospheric specifications to investigate how infrasonic propagation characteristics varied over the globe for a given universal time—in particular, how acoustic energy is partitioned among the tropospheric, stratospheric, and thermospheric ducts. Comparing infrasonic propagation characteristics computed with G2S atmospheric specifications and multiyear time series of observations, Antier et al. (2007) demonstrated that atmospheric specifications provided by operational numerical weather

predictions, such as the National Oceanic and Atmospheric Administration (NOAA) Global Forecast System (Kalnay et al. 1990) and the European Center for Medium-Range Weather Forecasts (Courtier et al. 1998), can accurately predict much of the day-to-day variability observed in infrasonic propagation characteristics. Additional discussion of related issues can be found in Drob et al. (2010a).

One of the outstanding issues is the observed variation in infrasonic propagation characteristics for thermospheric propagation, which results from planetary wave variability and day-to-day modulation of the upward-propagating, solar migrating and nonmigrating diurnal and semidiurnal tides. Current G2S atmospheric specifications are unable to resolve high-resolution atmospheric winds and temperatures above 75 km and thus must rely deterministically on empirical climatologies such as those from the combined Horizontal Wind Model (HWM07) and Naval Research Laboratory, Mass Spectrometer, Incoherent Scatter, Extended (NRLMSISE-00) models. The related issues, from an observational and modeling perspective, of examining in detail the local time and seasonal variations of repeating signals from the Tungurahua volcano are described in Assink et al. (2012).

Internal atmospheric gravity waves are a natural result of the buoyancy and stratification of the atmosphere. The basic linear theory of gravity waves is described in, for example, Holton (1992). A recent review of these interval waves, independent of their influence on infrasonic propagation, is provided by Fritts & Alexander (2003). These waves are excited by a wide range of sources in the lower and middle atmosphere, including cumulous convection, flow-over topography, and various dynamical instabilities. Gravity waves produce a red-noise spectrum of internal buoyancy oscillation throughout the atmosphere. Typical propagating gravity waves have vertical wavelengths anywhere from 1 to 60 km, horizontal wavelengths between 10 and 2,000 km, periods that range from 5 to 360 min, and horizontal phase velocities up to 90 m s^{-1}. There are three subclasses of gravity waves: acoustic-gravity waves, gravity waves, and inertio-gravity waves. These subclasses range from low to high frequencies, depending on the scale of the ratio of ω (intrinsic frequency) to the Brunt-Väisälä (BVF) frequency (high-frequency limit) and the Coriolis frequency (low-frequency limit) (acoustic gravity waves $\omega <$ BVF, gravity waves BVF $< \omega \ll$ Coriolis, and inertio-gravity waves BVF $\ll \omega <$ Coriolis). Typically originating in the lower atmosphere, these waves grow in amplitude with increasing altitude because of the exponential decrease in density with altitude. The wave amplitudes often saturate in the middle atmosphere from an overabundance of wave energy (Fritts & Alexander 2003). Near the mesopause, the waves can actually break owing to dynamical instabilities, at which point the wave action cascades to smaller scales, eventually becoming turbulence.

It has been acknowledged for at least a decade that synthetic modeling that does not account for gravity waves (i.e., synthetics are computed using smoothed models of sound speed in the atmosphere) fails to accurately reproduce observed waveform amplitudes and durations, both of which are important source discriminators. The importance of internal wave scattering of infrasonic energy in the stratospheric and thermospheric ducts has been identified (e.g., Chunchuzov 2004, Kulichkov et al. 2004, Ostashev et al. 2005, Millet et al. 2007), but the phenomenon is not fully understood. Such synthetics often illustrate multipathing that is commonly observed in recorded data, but the individual computed synthetic signals are most often simple pulses, lacking the durations and relative envelope amplitudes that have been seen so often in actual recordings. For example, these waves are known to be responsible for internal scattering of infrasonic energy into and out of ducts, as well as into the near-field shadow zone (a region where the sound pressures are predicted to be very low). In addition, the vertical wavelengths and amplitudes of these waves also cause infrasonic waveform complexity via the transient low-velocity zones that they generate (e.g., ReVelle 2010).

7.2. Infrasonic Wind Noise Problem

The main difficulty in measuring infrasound is the noise created by wind. Increasing winds correlate with increasing noise levels across the entire infrasonic band (see Walker & Hedlin 2010 and references therein). A simple wind noise experiment at the Piñon Flat Observatory in southern California comparing pressure power spectral densities recorded in various winds by a low-frequency microphone with a sponge filter placed 50 cm above the ground shows that in the 1–10-Hz range, the wind noise increases by approximately 5 dB per m s^{-1}. In lower-frequency bands, the increase in noise varies from 2 to 7 dB per m s^{-1} (McDonald et al. 1971, Hedlin & Alcoverro 2005). Typical infrasonic signals from remote and local sources range from 5 mPa to 5 Pa. A 50-mPa infrasonic signal clearly recorded in winds of 1 m s^{-1} would be completely masked in winds of 4–5 m s^{-1} without an effective wind filter.

There are generally thought to be several types of wind noise. The three main types that were introduced and investigated by Raspet et al. (2006) and Yu et al. (2011) are stagnation pressure fluctuation, turbulence-turbulence interaction, and turbulence–mean shear interaction. Stagnation pressure fluctuation noise occurs when the wind velocity blowing over a sensor is fluctuating. The stagnation pressure is the pressure that forms at the front of the sensor owing to the impact of the wind. Therefore, variations in wind velocity (due to turbulence) lead to measured variations in pressure. This type of wind noise should be reducible if the sensor surface area is large (e.g., via spatial averaging) or if the sensor is isolated from the stagnation pressure maximum (e.g., via wind fences or forests).

The second type of wind noise, turbulence-turbulence interaction, occurs during turbulence as air masses are chaotically colliding, shearing, and separating. These inertial interactions create pressure changes. Taylor's Frozen Turbulence hypothesis implies that these anomalies are "locked" in the mean air flow, further implying that such pressure anomalies are advected over an infrasonic sensor and recorded as noise. This type of noise is thought to be most important at higher frequencies and/or for sensors at least a meter above the ground.

The final type of wind noise, turbulence–mean shear interaction, is important on or close to the ground, where there is a significant vertical gradient of the mean horizontal wind speed. Horizontal changes in vertical velocities in turbulence cells interact with this vertical gradient in horizontal wind to create pressure anomalies. This type of noise is expected to be important throughout the infrasonic band for typical infrasonic sensors.

7.3. Infrastructure

To date, infrasonic research has been slowed by the lack of stations. The average distance between adjacent infrasonic arrays in the global network (the IMS) is 2,200 km. This distance is too sparse for the arrays to be used for detailed investigation of the fine-scale structure of infrasonic propagation. We know from many data and everyday experience that the atmospheric structure is changing continuously at considerably smaller scales that affect infrasonic propagation. This complex structure is undersampled and aliased by the IMS infrasonic array network. At regional distances, a single infrasonic station cannot be used to map out limits of infrasonic shadow zones or, equivalently, understand where branches of ducted infrasonic energy return to Earth's surface. In many instances, important geophysical details are below the resolving power of current infrasonic networks and even enhanced networks that will be developed in the foreseeable future. Trying to use existing infrasonic stations to map out an infrasonic wave field—i.e., sound pressure at ground level—from an event of interest is akin to the impossible task of fathoming the geological structure of an entire sedimentary basin given core samples from one or two drill holes. Without more

stations, we cannot accurately delineate infrasonic shadow zones or subject whatever atmosphere and infrasonic synthesis codes we develop to rigorous tests.

8. EFFORTS TO ADDRESS THESE ISSUES

Progress on these issues continues, and infrasound is used in an increasing number of diverse studies. In this section, we discuss a few key areas of research.

8.1. Modeling Atmospheric Structure

Because infrasonic transmission depends on the state of atmosphere, accurate infrasonic modeling requires the inclusion of all relevant physical mechanisms controlling infrasonic propagation—winds, adiabatic sound speeds, scattering, and attenuation and dispersion—and requires that variations in these values be correctly specified. An overview of the application of numerical methods to infrasonic monitoring may be found in Norris et al. (2010); here, we outline current research areas.

Infrasonic propagation at altitudes above 90 km remains poorly understood. A recent study of infrasonic signals from the terminal burst of a large bolide recorded at a dense network of 200 seismic stations distributed across 1,000,000 km^2 has revealed a set of thermospheric arrivals with frequencies above 2 Hz (Hedlin et al. 2010); it seems likely that these arrivals would be misidentified for a sparser network. However, a careful analysis of the arrival times and locations of these arrivals indicates that they are indeed consistent with thermospherically refracted arrivals but at much higher temporal frequencies than expected (de Groot-Hedlin et al. 2011). One factor obfuscating our understanding of infrasonic propagation at high altitudes is that ambient pressures and densities are extremely low; atmospheric pressure decreases exponentially, halving roughly every 5 km with altitude. Thus, the usual, linear assumption that the sound wave pressures and densities are negligible compared with ambient values may be incorrect, and nonlinear propagation may have to be taken into account in analyzing thermospheric returns. The frequency shift associated with nonlinear propagation may serve to explain the high frequencies seen by Hedlin et al. (2010) and de Groot-Hedlin et al. (2011). Another issue to be considered in propagation is the assumption that the atmosphere may be treated as a Newtonian fluid; this assumption is implicit in descriptions of atmospheric attenuation (Sutherland & Bass 2004, de Groot-Hedlin 2008). Instead, it is possible that the increasing ionization of the atmosphere at approximately 90 km significantly alters infrasonic propagation.

Unfortunately, the small-scale atmospheric structure is difficult, if not impossible, to resolve over all altitudes, at all times, over all latitudes and longitudes; however, its statistical effects on infrasonic propagation can be parameterized much in the same way that turbulence is parameterized in hydrodynamic calculations. For example, numerical weather prediction models for the middle atmosphere typically use spectral gravity wave parameterizations as described in Warner & McIntyre (1996) to parameterize the net statistical influence of these waves on the general circulation and large-scale ($>10^3$-km) meteorology. Recent theoretical studies on gravity wave parameterizations for infrasonic propagation have been presented by Chunchuzov (2004), Ostashev et al. (2005), and Gibson et al. (2010).

Recently, such waveform structure has been successfully modeled through the inclusion of stochastic representations of internal gravity waves in infrasonic waveform calculations (Gibson et al. 2010, Kulichkov et al. 2010). Studies in which gravity waves are added to the background profiles (e.g., G2S) have shown great promise in explaining the temporal complexity (frequency

content, signal amplitude, wave packet durations) seen in recorded data (e.g., Kulichkov et al. 2010, Green et al. 2011).

8.2. Numerical Modeling

Numerous different methods are used to model acoustic propagation. Ray methods (e.g., Jones et al. 1986, Garcés et al. 1998, Drob et al. 2003) that are applicable to acoustic propagation and refraction in an advected medium are often used to gain a first-order approximation to infrasonic propagation. Although ray theory is based on a high-frequency approximation to acoustic propagation, its value in modeling low-frequency infrasonic propagation has been confirmed by many studies (e.g., Le Pichon et al. 2005, de Groot-Hedlin 2008). The primary advantage of rays is that they offer rapid computation and a clear visualization of the infrasonic transmission paths, which is especially useful for source location purposes. The primary drawback is in the lack of accurate amplitude information; rays fail, for instance, to predict the infilling of shadow zones by low-frequency diffraction.

Increasing numerical accuracy is afforded by methods that have correspondingly greater computational load. Linear methods include the parabolic equation (PE) method, the finite-difference time-domain (FDTD) method, and the pseudospectral time-domain (PSTD) method. The PE method allows for advection (e.g., Lingevitch et al. 2002) but generally limits propagation to the forward-propagating wave, so that multiple scattering is ignored. The method is thus most appropriate for models with limited range dependence and those in which inhomogeneities are considerably larger than the wavelengths of the infrasonic energy. The FDTD method is a highly flexible tool for infrasonic propagation, because equations for the primary physics that governs propagation—including attenuation, dispersion, and winds—are directly incorporated into the method (de Groot-Hedlin 2008, de Groot-Hedlin et al. 2010). Because the FDTD method is a full-wave method, it allows for small-scale scattering, as well. Its primary drawback is in the computational load; the choice of spatial and temporal discretization is crucial to obtaining a stable result. The PSTD method, an enhancement of the FDTD method, requires only two spatial points per wavelength, greatly reducing the storage and computation time (Hornikx et al. 2010).

Nonlinear propagation modeling is a key research area in infrasonics. Nonlinear effects arise for large sources and for acoustic propagation to exceedingly high altitudes where the atmospheric pressure is exceptionally low. In these cases, the pressure perturbation associated with the passage of the acoustic wave may be a significant fraction of the ambient field. This gives rise to a shift in energy from lower to higher frequencies, distorting the waveforms and altering the attenuation characteristics. Although the key equations governing nonlinear infrasonic propagation have been developed (Wochner et al. 2005), numerically solving these equations for realistic atmospheric models remains a challenge.

8.3. Filtering Wind Noise

As mentioned above, even mild winds can easily deafen infrasonic sensors. Although it is advantageous to place infrasonic sensors in forests or beneath snow owing to the inherent protection from the wind, there are many locations of interest where doing so is impossible. This limitation has fueled research in methods to reduce wind noise. One of the most successful approaches has been to make spatial averages of pressure measurements. Infrasonic wave fronts have correlation distances of roughly a few wavelengths, depending on the nature of the source and propagation path. For 1 Hz, the correlation distance is roughly 1 km. Pressure anomalies associated with turbulence have a coherence length that is proportional to wind speed and turbule size (e.g., Shields 2005). If

atmospheric pressure is sampled at a number of locations (n) spaced far enough apart so that the pressure variations from wind noise are uncorrelated, but close enough so that the acoustic signal remains coherent and in phase, summing the time series increases the noise power by n and the signal power by n^2, resulting in a signal-to-noise improvement of $10\log_{10}(n)$ dB. This led to the Daniels filter—a series of tapered pipes with sensing inlets distributed uniformly along its length and a microphone connected to its wide end (Daniels 1959). The filter is designed to improve the signal-to-noise ratio of coherent infrasound as it propagates from the narrow end to the wide end through the length of the tapered pipes. Provided that $rf^{1/2}$ is greater than ~0.1 m-s$^{1/2}$, where r is the pipe radius and f is the signal frequency, the wave speed inside the pipe will match the wave speed outside, and the signals inside the pipe will sum in phase provided the narrow end of the pipe is pointing directly toward the source. Whereas the filter sums the signal in phase, incoherent noise from the inlets that travels acoustically inside the pipe is attenuated owing to the scaling.

The Daniels filter is a line microphone. This is important because infrasound typically propagates along Earth's surface at grazing elevation angles. The filter has an omnidirectional infrasonic response for wavelengths larger than four times the length of the filter. For shorter wavelengths, the response is anisotropic and a function of signal back azimuth (Daniels 1959, Cook & Bedard 1971).

A rosette filter, the standard filter used by the IMS, is an extension of the Daniels filter and comprises a spatial array of solid pipes that are interconnected to a central microbarometer or low-frequency microphone (**Figure 4**). The original rosette design comprises 32 low-impedance inlets arranged in a geometrically regular pattern around a 16-m-diameter circle and connected by solid

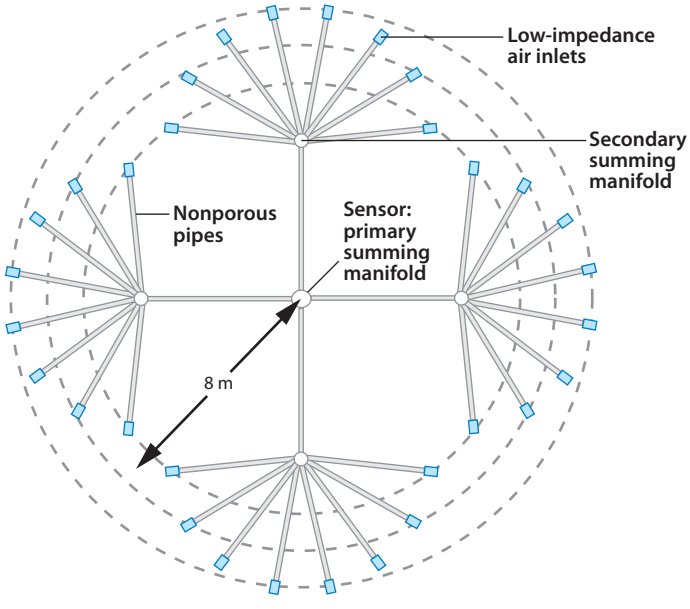

Figure 4

Prototype rosette noise-reduction filter. The salient feature of this filter is that signals and noise are summed at a microbarometer located at the center of the filter after an identical propagation time delay from the inlets for vertically incident wave fronts. Most infrasonic wave fronts, however, graze Earth's surface. Redrawn with permission from Alcoverro & Le Pichon 2005 (Alcoverro B, Le Pichon A. 2005. Design and optimization of a noise reduction system for infrasonic measurements using elements with low acoustic impedance. *J. Acoust. Soc. Am.* 117:1717–27). Copyright 2005, Acoustic Society of America.

pipes to a microbarometer where sound from all inlets is acoustically summed. The along-pipe distances from all inlets to the microbarometer are equal, and thus, at any moment, pressure at the microbarometer is the sum of pressure changes that entered each inlet of the filter simultaneously.

The rosette has an omnidirectional response to infrasound. Infrasound usually propagates at grazing angles to the ground. Therefore, signals with wavelengths that are twice the diameter of the rosette destructively interfere at the central microbarometer. Although this omnidirectional response permits using standard array-processing techniques to determine signal back azimuth and trace velocity, it puts a limit on the maximum wind noise reduction that can be achieved by any rosette. Larger filters provide a greater separation of inlets to attenuate the noise from wind turbulence better via averaging, but such larger filters also attenuate true infrasound that propagates across all the filter inlets. Designs used at IMS sites range in diameter from 18 to 70 m, with considerably more inlets. In tests at the Piñon Flat Observatory, Hedlin et al. (2003) found that in winds up to 5.5 m s^{-1}, the 18-m rosette with 96 inlets reduced noise by as much as 20 dB above 0.2 Hz; a 70-m rosette reduced noise by a similar amount, between 0.02 and 0.7 Hz. The other disadvantages of rosettes are that they are subject to significant and problematic resonance (Hedlin & Alcoverro 2005) and that they are large and time-consuming to build and maintain.

Irrigation soaker hoses have also been used as wind filters. Pressure variations from both spatially coherent infrasound and spatially incoherent wind turbulence propagate through the pores, providing some level of signal-to-noise improvement at the summing microbarometer (e.g., Marston & Gabrielson 2008). These filters are commonly used at temporary recording sites, where the goal is to record for a relatively short period of time (e.g., days to weeks/months) for a relatively low cost. Although the filters are inexpensive, they are thought to suffer from an unpredictable impulse response owing to different manufacturers, age of the hose, and degree of solar exposure. More importantly, the level of achievable wind noise reduction is also limited, as it is with rosettes.

Whereas the previous filters rely on acoustic summation of signals traveling through pipes, the Optical Fiber Infrasound Sensor (OFIS)—a sensor that is, by design, also a wind filter—achieves wind noise reduction via spatial averaging along a line (Zumberge et al. 2003). The OFIS is a compliant, sealed tube that instantaneously averages pressure variation along its length by interferometrically sensing pressure-induced diameter change, which naturally obviates resonance in the pressure recordings. An OFIS can be oriented in different ways. Although one can simply use circular OFISs as array elements and avoid any change to standard array-processing software, a circular OFIS attenuates infrasound by approximately the same amount as does a rosette of the same diameter (**Figure 5**). The optimum orientation for reducing wind noise while preserving infrasonic signal fidelity is a straight line. In this directional-microphone configuration, the level of noise reduction and signal-to-noise ratio improvement for signals broadside to the sensor is simply a function of length. Although more advanced array-processing techniques have been developed to exploit the OFIS directionality to determine signal back azimuth for several signal recordings by OFISs in different orientations (Walker et al. 2008), one could also make relatively minor changes to standard array-processing algorithms for use with several OFIS clusters, in which each cluster comprises several OFISs in a radial wagon-wheel configuration. With such a configuration, one can make very long OFISs to achieve a desired level of omnidirectional signal-to-noise improvement in windy areas. Recent experiments at the Piñon Flat Observatory have shown that a 270-m-long OFIS provides a signal-to-noise improvement of ~10 dB at 1 Hz relative to all rosette elements of the colocated IMS array. Furthermore, the improvement increases with increasing frequency and wind speed.

Other solutions to wind noise have been proposed, including the use of wind fences and enclosures (Hedlin & Raspet 2003, Liszka 2008), dense sensor arrays, and rigid porous media.

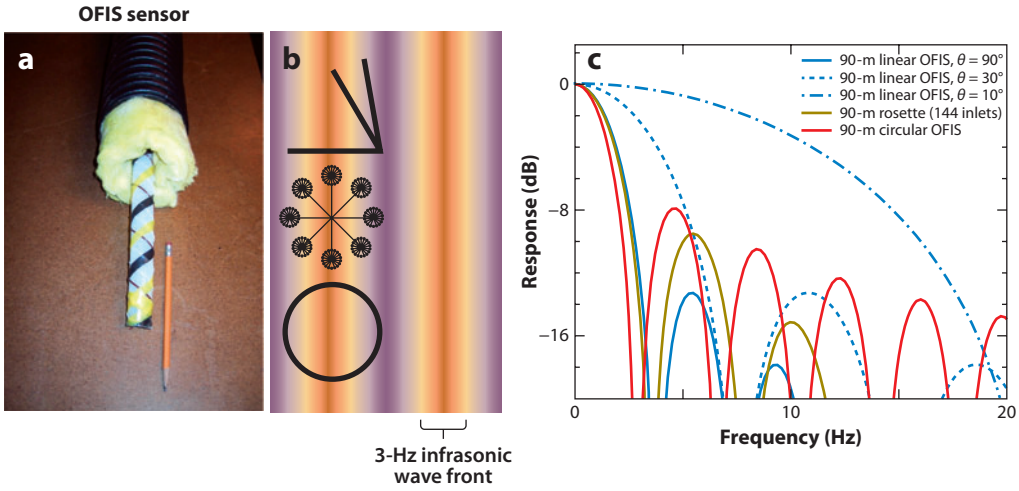

Figure 5

Instantaneous averaging of pressure along a line provides a level of wind noise reduction that can be increased with increasing length and without attenuating broadside infrasonic signals. (*a*) Photo of an Optical Fiber Infrasound Sensor (OFIS) sensor, with a pencil for scale. (*b*) Map view comparison of a circular OFIS (*bottom*), a rosette (*middle*), and three linear OFISs with different azimuths relative to an infrasonic wave front. (*c*) Responses of the different sensors and wind filters in panel *b*. A node exists near 3 Hz for the rosette, circular OFIS, and linear OFIS oriented perpendicular to the wave front.

More work appears necessary to determine if any of these methods provides a level of improvement beyond that provided by spatial averaging. The result of this research will likely determine the success of infrasonic arrays in the IMS network that are required by treaty to be located on small, windy islands.

8.4. Sampling: Infilling the Infrasonic Network with Seismometers

The infrasonic network is too sparse to be used for detailed investigation of the fine-scale structure of infrasonic propagation. We have a poor understanding of the geographic and temporal distribution of many infrasonic sources that are large but not large enough to trigger several stations in the IMS network. More stations are needed. Recent studies suggest that we can significantly improve our understanding of infrasonic propagation and expand studies of infrasonic sources, their physics, and their geographic distribution by using existing seismic stations rather than investing in new infrasonic monitoring stations. It is now well established that seismometers can be useful infrasonic sensors (e.g., Kanamori et al. 1991). In many regions, existing seismic stations provide much-needed dense sampling of the infrasonic wave field.

To illustrate, we give an example from the western United States in 2007–2008, when the 400-station broadband USArray Transportable Array stretched 700 km east from the Pacific coast and north–south between the Canadian and Mexican borders. Using reverse time migration applied to envelopes of band-pass filtered vertical component data, Walker et al. (2011) located several hundred atmospheric sources each year in the western United States (**Figure 6**). The atmospheric sources are clustered in Nevada, Utah, Idaho, and California, defining what are termed infrasonic hotspots. Many of these events are not seen by any of the infrasonic arrays in the region, further demonstrating the richness of the infrasonic wave field between globally spaced arrays.

The seismic data permit study of infrasonic propagation in unprecedented detail. **Figure 7** shows one typical example of infrasonic branches clearly seen in the seismic data. This example

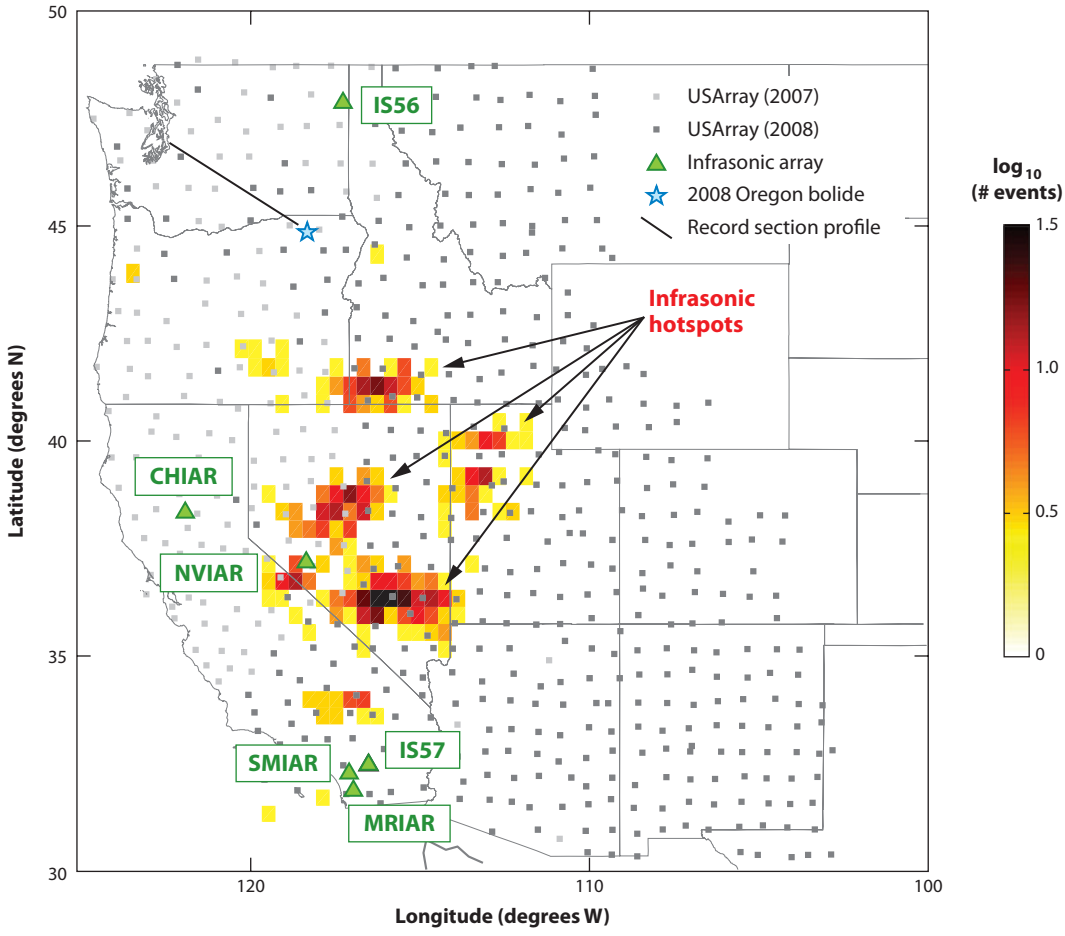

Figure 6

Seismic stations in the USArray Transportable Array during 2007 and 2008. A bolide burst in 2008 at an altitude of 27 km above northeast Oregon. An east–west record section of the acoustic-to-seismic signals from this event shows multiple infrasonic arrivals in unprecedented definition, requiring a new nomenclature for infrasonic arrival ray paths (Hedlin et al. 2010). Approximately 900 other events have been located using the full 2007–2008 USArray data set (Walker et al. 2011). Color indicates the relative density of these located events, defining what are termed infrasonic hotspots. Modified from Walker et al. (2011).

is from a focused study of a single bolide that burst 27 km above northeast Oregon (Walker et al. 2010) (**Figure 6**); the profile is located along the heavy line to the northwest of the source. Two branches of infrasonic signals can be clearly seen. Modeling conducted by Hedlin et al. (2010) showed that the early branch is an amalgamation of signals that propagated directly down from the bolide or up from the source and then refracted back to the ground in the stratospheric duct. The later branch was ducted in the stratosphere after being emitted down from the source and reflecting from the free surface. The full extent of these branches could not be fathomed using existing infrasonic stations, which could be used only to spot-check the infrasonic wave field. The seismic stations give much tighter constraints on the range at which the branches emerge from shadow zones (**Figure 2**), the manner in which the character of the signals changes with range, and the location at which each branch fades again at greater range.

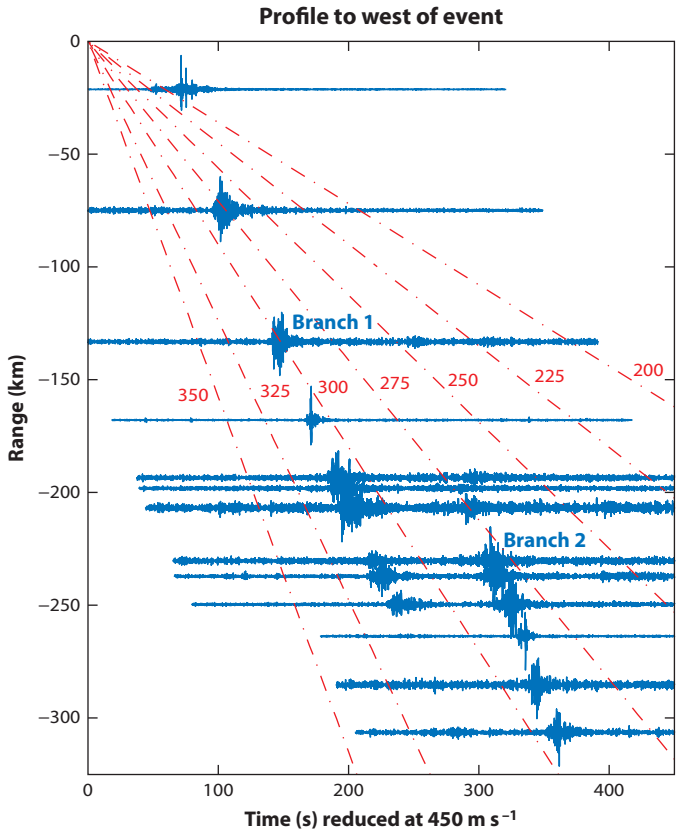

Figure 7

Record section showing acoustic-to-seismic coupled signals from the Oregon bolide (**Figure 6**). The dense seismic network data permit study of entire branches of acoustic signals. The branches are from the bolide directly down to the ground (Branch 1) and ducted in the stratosphere after reflecting from the ground (Branch 2). The red dashed lines give celerity in m s^{-1}. From Hedlin et al. (2010).

Insights into propagation can also come from the statistical analysis of acoustic-to-seismic recorded signals originating from hundreds of infrasonic events. Simply analyzing the optimum celerity (horizontal distance traveled divided by time of travel) of the catalog of 901 infrasonic source locations, Walker et al. (2011) found evidence suggesting that the predominant infrasonic energy at the surface in the western United States is in the form of ducted stratospheric arrivals with a celerity range between 275 and 305 m s^{-1}. Furthermore, the authors document a seasonal variation in signal celerity that exhibits a good correlation with variation in atmospheric temperature. This observation reminds us that signal celerity by itself is a poor indicator of the turning-ray height; the latitude range spanned by propagation and the season are important influences simply through atmospheric temperature.

Although recent observations suggest that seismometers may sometimes be less affected by wind noise than are infrasonic sensors, waveform interpretations of seismic data must be performed carefully because of complexities that can arise during the conversion of acoustic energy to seismic energy. Future studies of arrays of colocated acoustic and seismic sensors will illuminate the details of this complexity and provide a better understanding of the limitations of seismic data for infrasonic research.

9. SOURCE PHYSICS PROBLEMS

Infrasound has been proposed to result from a variety of geophysical phenomena (e.g., Campus & Christie 2010). Such phenomena include earthquakes, tsunamis, volcanoes, landslides, meteors, lightning and sprites, auroras, and oceanic-atmospheric dynamics. We focus on five of the most frequently studied sources: auroras, meteors, earthquakes, microbaroms, and volcanoes.

9.1. Auroras

Traveling pressure waves associated with geomagnetic activity were first reported in detail by Chrzanowski et al. (1961) and given rigorous mathematical treatment by Maeda & Watanabe (1964). Observations documenting the phenomena with simultaneous measurements by all-sky auroral imagers, radars, magnetometers, and ground-based infrasonic sensors are described by Wilson (1975).

Two generating mechanisms have been hypothesized for low-frequency (<0.1-Hz) infrasonic signals associated with auroras. Aurora infrasound waves are often impulsive infrasonic signals generated by supersonic motion of auroral arcs that contain strong electrojet currents; this motion sets up a shock wave large enough to be observed on the ground (Wilson et al. 2005, de Larquier et al. 2010). A newer hypothesis is that pulsating aurora infrasound waves are generated by the heating of the atmosphere (by the precipitation of auroral electrons) within pulsating auroral patches in thin layers of the lower ionosphere. These quasi-continuous signals often have durations of hours, have amplitudes of 50–200 mPa, and are observed with high trace velocities (Wilson et al. 2005).

9.2. Meteors

Meteors generate infrasound as they tunnel through the atmosphere at hypersonic velocity and explosively fragment along their trajectory. Numerous studies have used seismic recordings of the acoustic-to-seismic coupled signal associated with the shock wave to estimate meteor trajectories (Ishihara et al. 2003, Langston 2004). These studies performed a grid search to minimize the difference between observed and predicted travel times for the six-parameter source model assuming a constant atmospheric sound velocity.

Some meteors are characterized by a brilliant terminal burst or several large bursts along the trajectory, and infrasound has been used to determine the source times and locations of these events (e.g., Arrowsmith et al. 2007). These studies also relied on picked arrival times of seismic recordings of the acoustic-to-seismic coupled signals from the bursts.

A different approach was taken by Walker et al. (2010) to locate the terminal burst associated with the Oregon 2008 bolide. They analyzed the full waveforms of hundreds of USArray and Incorporated Research Institutions for Seismology (IRIS) Program for Array Seismic Studies of the Continental Lithosphere (PASSCAL) seismic stations in the western United States by using reverse time migration with a constant-velocity model as well as a grid search to minimize the misfit between observed and synthetic arrival times predicted by 3D ray tracing.

A precise thermoacoustic model for infrasonic generation from meteors has not been established. Methods used to locate infrasonic sources from meteors often require an assumption about how the energy was radiated from the meteor (from either a point source or a continuous emission of infrasound from along the trajectory). However, care must be taken that such assumptions and subsequent locations do not bias resulting interpretations of the source physics. For example, many meteors may not exhibit a distinct flash during the entry, which can lead one to

automatically consider the more complex hyperbolic trajectory model rather than a point source to explain any anomalous infrasound. However, even in these cases, depending on the source physics and on the source-receiver geometry, a point-source model may predict the observations nearly as well as a hyperbolic trajectory model does. Indeed, comparing the fits of the data to both model types provides useful information for studying and testing source physics hypotheses. Perhaps source-imaging methods using meteor infrasonic recordings made by relatively dense arrays of microphones will image the amplitude distribution of the infrasonic radiation along the trajectory, free of a priori assumptions about the source model or concerns about errors in picked arrival times.

9.3. Earthquakes

Earthquake infrasonic source physics is still in its infancy. Earth's surface is a speaker [Rayleigh 1945 (1896)]. There have been several studies of global infrasonic emissions owing to very large strike-slip earthquakes (e.g., Mikumo 1968, Olson et al. 2003) and subduction-zone earthquakes (e.g., Le Pichon et al. 2006b). Le Pichon et al. (2006b) associated these observations with mountain and/or ground displacements in the greater epicentral region. A pivotal study by Le Pichon et al. (2003) established that the strike-slip Kokoxili 2001 earthquake (Mw 7.8) radiated infrasound in the 0.05–1.0 Hz band that was detected at 1,800-km range by an infrasonic array in Mongolia (**Figure 8**). Assuming that linear topographic features are directional speakers, they forward-modeled the locations of the launch points of the seismic-to-acoustic converted infrasonic rays that were predicted to ensonify the Mongolia array. They found that these predicted locations correlate fairly well with the locations of observed arrivals that are back-projected to their source locations assuming a constant celerity.

The relative contributions of infrasonic emission due to excited topographic features and that due to flat areas remain to be accurately quantified. On the one hand, mountains extend higher into the troposphere, providing a greater potential for injecting infrasound into the atmosphere at a low enough ambient sound speed (decrease of 4 m s^{-1} per km altitude) to provide returns to the ground at distant ranges. Mountains also can be directional, which helps radiate loud infrasound at relatively shallow elevation angles, facilitating injection into a stratospheric duct. On the other hand, owing to the decrease in air density with increasing altitude, for a given vertical displacement of a flat surface, the pressure perturbation at sea level is a factor of 2 greater than it would be at ~7-km altitude. This nondirectional, upward-radiated infrasound would encourage thermospheric ducting, especially if the initial surface pressure was large enough such that propagation in the thermosphere was nonlinear. A pioneering study by Mutschlecner & Whitaker (2005) addressed part of this question. They analyzed 31 stratospherically ducted infrasonic signals from regional and teleseismic earthquakes recorded over a 20-year period by three arrays in the western United States. The authors showed that signal amplitude in the 0.5–3-Hz band, after applying a correction term for stratospheric wind and spherical spreading, exhibits a fair correlation with seismic earthquake magnitude and surface velocity in the epicentral region. Because these earthquakes were from regions with different densities and shapes of topographic features and because the signals were recorded by different arrays, the simplest interpretation is perhaps that the vertical acceleration in the epicentral region by Rayleigh waves generated the observed stratospheric arrivals. Although the correlations are clear, there is still quite a bit of variance. The authors showed that the most sensitive parameters in these correlations are the mean stratospheric wind between the source and receiver used in the amplitude correction and the variance in the surface velocity with magnitude. The authors also found a good correlation between earthquake magnitude and infrasonic signal time duration. They hypothesized that the signal duration is simply proportional to the surface area around the epicenter that is vertically excited beyond a threshold amplitude.

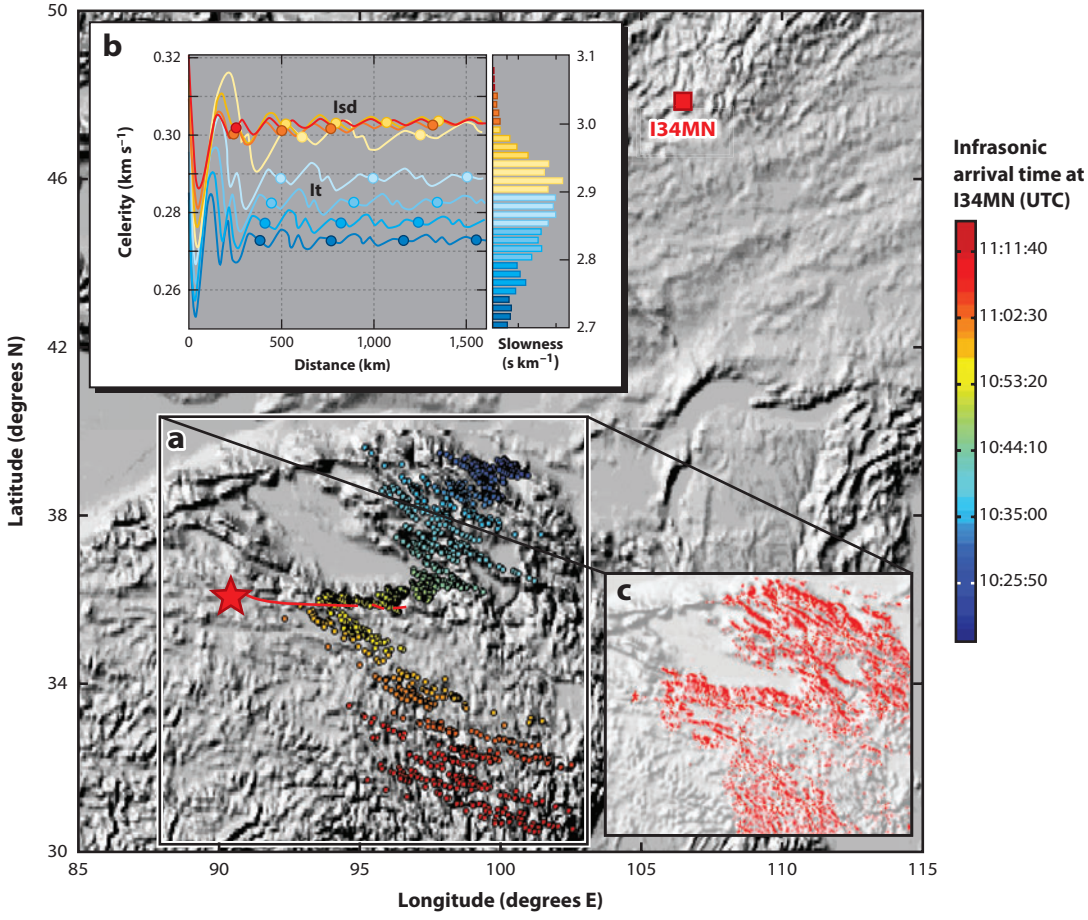

Figure 8

Comparison of predicted and observed infrasound from the 2001 Kokoxili earthquake recorded by International Monitoring System (IMS) array I34MN. (*a*) Locations of launch points for back-projected infrasonic rays assuming a constant celerity and instantaneous launch time. (*b*) Predicted variation of actual celerities for the different launch points, showing that a stratospheric celerity is generally appropriate. (*c*) Locations of launch points that generate energy predicted to ensonify the array. Abbreviations: Isd, stratospherically ducted; It, thermospheric; UTC, Coordinated Universal Time. From Le Pichon et al. (2003).

Additional fluid-dynamics modeling studies incorporating seismic rupture models and associated radiation patterns, especially with additional infrasonic stations and at higher infrasonic frequencies where noise is less problematic, will no doubt improve our understanding of the physics of seismic-to-acoustic coupling in regions excited by earthquakes. This possibility, of course, has a much broader impact. Such a study is pertinent to the generation of the U.S. Geological Survey's ShakeMaps, the primary component of the PAGER (Prompt Assessment of Global Earthquakes for Response) system, which predicts the human impact due to significant earthquakes around the world and is utilized by emergency responders, government agencies, and the media (Wald et al. 2010). Specifically, if infrasonic recordings can be used to reliably measure the amplitude of surface shaking, their strategic positioning near heavily populated, tectonically active areas that are not sampled well by strong-motion seismometers may provide a useful data set for the generation of ShakeMaps. Even for areas that are well sampled by a strong-motion network, such infrasonic

data might still be useful for the purposes of accurate interpolation of shaking estimates between seismic stations, perhaps removing the necessity of an assumed earthquake rupture model.

9.4. Microbaroms

Benioff & Gutenberg (1939) observed quasi-continuous atmospheric pressure oscillations that they termed microbaroms, which had rather large amplitudes on the order of 100 mPa and a central period of ~4–8 s. Gutenberg & Benioff (1941) showed that microbaroms are similar to microseisms, which usually are observed as Rayleigh waves but also are present in Love and compressional waves (Haubrich & McCamy 1969). However, microseisms are observationally different in that they typically are peaked at 5 and/or 10 s (Gutenberg 1958).

The leading hypothesis to explain microbaroms and microseisms is that they are generated by the same standing ocean waves owing to the interaction of two antiparallel ocean swells with the same period (Rind 1980). Seismically, the standing ocean waves impart displacements of the seafloor owing to a second-order nonlinear term for pressure that does not decrease with depth and has a magnitude proportional to the product of the two antiparallel swell heights (Longuet-Higgins 1950). Acoustically, these submarine pressure variations leak through the ocean surface into the atmosphere and explain ~80% of the atmospheric microbarom wave field (Brekhovskikh et al. 1973, Waxler & Gilbert 2006). The remaining ~20% of the wave field is explained by direct compression of the air above standing ocean waves (Daniels 1952, Arendt & Fritts 2000, Waxler & Gilbert 2006). The amplitude of both of these acoustic components is also proportional to the product of the energy of the opposing wave trains. This hypothesis implies that antiparallel swells in the deep ocean basins may contribute to the generation of global microbarom and microseism energy. Longuet-Higgins (1950) further showed that standing waves are likely to be amplified in some areas for special combinations of frequency and water depth in which compression waves can resonate between the seafloor and free surface. Therefore, this hypothesis also suggests that reflected swell from coastlines can interfere with the incident swell to create standing waves and nearshore microbarom/microseism energy radiation.

Microbaroms are almost ubiquitous in recordings by IMS infrasonic arrays. Although some IMS stations observe microbaroms continuously, the microbaroms are predominantly observed from October through March by boreal stations and from April through September by austral stations (e.g., Daniels 1952, Donn & Rind 1971, Le Pichon et al. 2009). A correlation exists between the seasonal variation in the zonal stratospheric winds and the microbarom amplitudes/azimuths at six IMS infrasonic arrays (Le Pichon et al. 2006a). In the Northern Hemisphere, microbaroms generally are detected from sources east of the arrays during the boreal summer and west of the arrays during the boreal winter. In the Southern Hemisphere, microbarom detections from eastern sources occur during the austral summer and from western sources during the austral winter. With regard to the seasonally varying zonal stratospheric winds, it would appear that for most of these cases the vector from the source to the arrays has a component in the stratospheric downwind direction. Furthermore, a good correlation was found between the number and amplitude of the detected infrasonic signals and the maximum stratospheric wind speed, further suggesting that most of the observed energy was due to the seasonally varying stratospheric duct.

Within this seasonal pattern, detection of these signals can be modulated by wind noise and diurnal variations in atmospheric propagation conditions (Tabulevich 1995, Kulichkov et al. 2004). In fact, the variation of microbaroms can be used to invert for upper atmospheric wind and temperature (e.g., Donn & Rind 1971, Garcés 2004, Le Pichon et al. 2005, Drob et al. 2010b), which is useful because current upper atmospheric wind models do not include global-scale planetary waves, interseasonal variability, and nonmigrating tides.

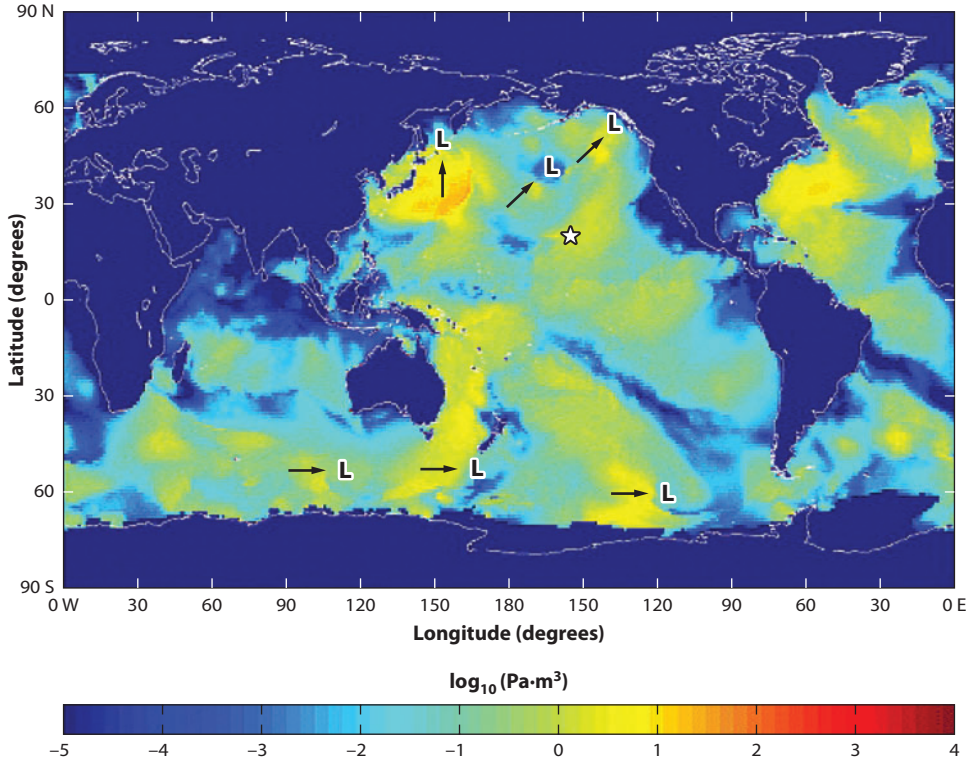

Figure 9

Magnitude of acoustic source pressure spectrum [$\log_{10}(\mathrm{Pa} \cdot \mathrm{m}^3)$] at 0.2 Hz due to opposing swells with a 10-s period on January 4, 2003, at 18:00 Universal Time. The white star indicates the Hawaii infrasonic array location (IS59), the letter L indicates a low-pressure center, and arrows indicate storm propagation directions. From Willis et al. (2004).

The microbarom source hypothesis also predicts potential sources in the deep ocean owing to routine wave activity or an excited sea surface associated with a passing atmospheric depression. Theory and observations suggest that a depression that travels faster than the group velocity of the self-generated swell will create a wake inside which newer swells interfere with the older swells that were initially set up in front of the depression (e.g., Longuet-Higgins 1950, Haubrich & McCamy 1969). Specifically, Willis et al. (2004) analyzed two years of infrasonic data recorded in Hawaii and found that microbaroms in the boreal winter months had an amplitude that was an order of magnitude larger than those in the boreal summer months, suggesting that predominant microbarom radiation follows the boreal and austral winters. Using the theory in Arendt & Fritts (2000) with NOAA Wave Watch III model directional wave spectra, Willis et al. (2004) computed the predicted global microbarom source strength at the sea surface (**Figure 9**). The predictions suggest significant microbarom radiation in the wake of the north Pacific depressions, although significant radiation is also predicted at great distances from depression centers. Focusing on an infrasonic array recording on the island of Palau, Hetzer et al. (2008) demonstrated a correlation between the location of observed infrasound and the location of opposing swells predicted by Wave Watch III models due to a west Pacific typhoon. This study was particularly noteworthy in that the array data unambiguously point to the region of opposing swells, which is at a much

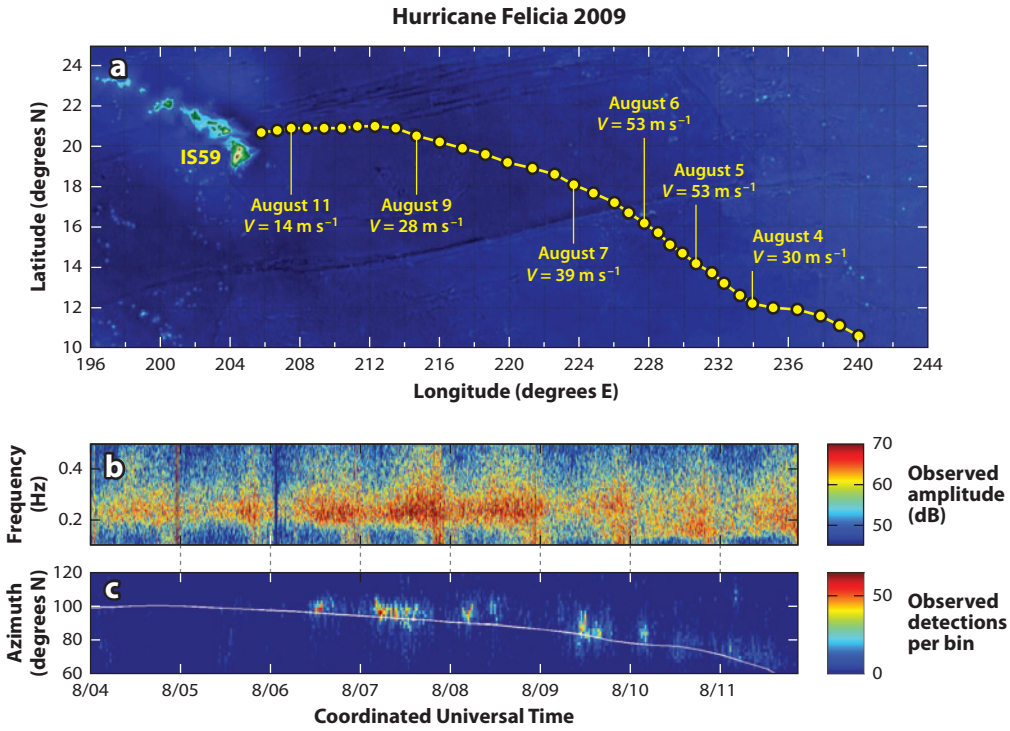

Figure 10

Correlation of infrasound observed in Hawaii with the approach of Hurricane Felicia in August 2009. (*a*) Track of storm center. (*b*) Infrasonic spectrogram recorded by one of the Hawaiian sensors. Amplitude is in dB with respect to 20 uPa^2 Hz^{-1}. (*c*) Density of detections (pixels) at the array as a function of time and back azimuth, with azimuth to the storm center shown for comparison. Modified from Stopa et al. (2011).

different azimuth than the region of greatest significant wave height, clearly showing that the latter is not useful for predicting microbarom/microseism radiation. Stopa et al. (2011) focused on the infrasound recorded in Hawaii (IS59) that was generated by Hurricane Felicia (**Figure 10**). They modeled the microbarom radiation of idealized depressions using the theory presented in Waxler & Gilbert (2006). They predicted and observed that the region of high opposing swell density moves from the eye of a stationary depression to the wake of a moving depression. They also predicted an exponential relationship between hurricane category and microbarom source amplitude that is unaffected by the physical size of the hurricane, suggesting that microbarom observations can be used to estimate the strength of a hurricane.

There is a natural synergy between microseisms and microbaroms. Although many microseism investigations have investigated the fine details of microseism source phenomena in the deep oceans and near coastlines, there have been relatively few microbarom studies and even fewer studies that combine observations of the seismic and infrasonic wave fields. Two factors that can help eliminate this gap in knowledge are making IMS infrasonic array data publicly available and analyzing dense networks of infrasonic pressure sensors such as the acoustic component of the USArray Transportable Array (TA). The advantage provided by the TA is that both infrasonic and seismic wave fields are being recorded by colocated sensors, enabling the use of identical techniques on both wave fields to investigate the physics of the source or the deviations in the infrasonic signals due to variations in atmospheric velocity structure.

9.5. Volcanoes

Volcanoes have traditionally been studied with seismology, geodesy, remote sensing, geochemistry, and geology to address academic questions as well as improve monitoring and detection capabilities. Over the past two decades, it has been established that near-field (within ~10 km) infrasonic and low-frequency acoustic sensor networks provide a reliable means for detecting and monitoring explosive eruptions (Garcés & Hansen 1998; Ripepe & Marchetti 2002; Johnson et al. 2003; Matoza et al. 2007, 2008). As was shown by Matoza et al. (2007), the January 2006 Mount St. Helens ash eruption emitted strong levels of infrasound that were clearly detected at a range of 13 km in the absence of a corresponding seismic signal. Furthermore, because the eruption occurred at night while obscured to satellites by cloud cover, the only other evidence that an eruption occurred was the loss of radio contact with U.S. Geological Survey instruments deployed in the summit region and the observation of local ash deposits the following morning. The seismicity before and during the eruption exhibited no remarkable differences. Even in cases in which volcanic processes give rise to detectable near-field seismic and acoustic signals, the seismic signals are more challenging to interpret because of scattering and attenuation along the source-receiver path. Listening to the sound field radiated by volcanoes has the potential to improve our understanding of volcanic processes that involve surface deformation transients and atmospheric injections as well as vastly improve our hazard detection and monitoring networks.

The general working hypothesis for infrasound generated by Strombolian, Vulcanian, or Plinian volcanic eruptions originates from several scholars (e.g., Garcés & McNutt 1997, Ripepe & Marchetti 2002, Matoza et al. 2009). Depending on magma viscosity, fluctuations in the velocity of magma flow give rise to seismic tremor at relatively greater depths of the volcanic conduit. The moving magma triggers melt injection and an associated explosion at relatively shallow depths owing to gas expansion/accumulation within the metastable magma or gas slug. Larger overpressures and supply volumes will lead to higher ejection velocities and longer eruption durations, respectively. In such cases, the eruptive column will radiate strong- and long-duration infrasound that, at local and regional distances, will exhibit spectral similarities to aircraft jet engine noise. Smaller overpressures and supply volumes will lead to slower ejection velocities and shorter durations. In these cases, the initial event may set up Helmholtz and acoustic cavity resonance and associated infrasound.

The seismic-to-acoustic transmission phenomenon can also generate infrasound owing to earthquakes beneath a volcano. In such cases, infrasonic and seismic energy in the near field will have similar characteristics but be separated in time owing to the difference in acoustic and seismic velocities. For example, Matoza et al. (2009) showed a fair correlation in waveform character between time-advanced infrasonic arrivals and seismic arrivals from activity beneath Mount St. Helens. Although they proposed several mechanisms to explain these "twins," including seismic-to-acoustic coupling, they found that there were extended durations of time when the infrasonic component "turned off." As they indicated, variations in atmospheric conditions, especially wind, may explain variations in such twin detection. This result highlights the additional complexity of using infrasound at regional and global distances to study volcano processes; such studies require waveform modeling using 3D atmospheric velocity models.

10. CONCLUDING COMMENTS

Infrasonics is seismology's close cousin and is emerging from its own nascent stage, just as seismology did several decades ago. During the earliest stages of seismology, it would have been difficult, if not impossible, to imagine how much that field would one day further our

understanding of the physics and structure of our planet's interior. Just as seismologists have spent decades tackling significant engineering and scientific issues to improve the quality of seismic data and the interpretation of the signals that seismometers record, the infrasonic community is making steady progress in interpreting infrasonic data. With continued growth, infrasonics may emerge as one of the key methods to probe our atmosphere and monitor its dynamics. It may also become an essential partner with seismology as we strive for a more complete understanding of the 3D seismoacoustic processes active near Earth's surface and the coupling by which signals or noise transmit from one medium to another. Just as an array of instruments on the surface of Earth or in orbit about the planet are now used to refine our understanding of the universe, the new infrasonic network will give us an unprecedented opportunity for an improved understanding of our planet.

DISCLOSURE STATEMENT

The authors are not aware of any affiliations, memberships, funding, or financial holdings that might be perceived as affecting the objectivity of this review.

ACKNOWLEDGMENTS

D.P.D. acknowledges support provided by the Office of Naval Research. K.W. and M.A.H.H. acknowledge support provided by the National Science Foundation under contract EAR-1053576.

LITERATURE CITED

Alcoverro B, Le Pichon A. 2005. Design and optimization of a noise reduction system for infrasonic measurements using elements with low acoustic impedance. *J. Acoust. Soc. Am.* 117:1717–27

Antier K, Le Pichon A, Vergniolle S, Zielinski C, Lardy M. 2007. Multiyear validation of the NRL-G2S wind fields using infrasound from Yasur. *J. Geophys. Res.* 112:D23110

Arendt S, Fritts DC. 2000. Acoustic radiation by ocean surface waves. *J. Fluid Mech.* 415:1–21

Arrowsmith SJ, Drob DP, Hedlin MAH, Edwards W. 2007. A joint seismic and acoustic study of the Washington State bolide: observations and modeling. *J. Geophys. Res.* 112:D09304

Arrowsmith SJ, Hedlin MAH. 2005. Observations of infrasound from surf in southern California. *Geophys. Res. Lett.* 32:L09810

Arrowsmith SJ, Johnson JB, Drob D, Hedlin MAH. 2010. The seismoacoustic wavefield: a new paradigm in studying geophysical phenomena. *Rev. Geophys.* 48:RG4003

Assink JD, Waxler R, Drob DP. 2012. On the sensitivity of infrasonic traveltimes in the equatorial region to the atmospheric tides. *J. Geophys. Res.* 117:D01110

Bass H, Bhattacharyya J, Garcés M, Hedlin MAH, Olson J, Woodward R. 2006. Infrasound. *Acoust. Today* 2:9–19

Benioff H, Gutenberg B. 1939. Waves and currents recorded by electromagnetic barographs. *Bull. Am. Meteorol. Soc.* 20:421–26

Brekhovskikh IM, Goncharov VV, Kurtepov VM, Naugol'nykh KA. 1973. The radiation of infrasound into the atmosphere by surface waves in the ocean. *Atmos. Ocean. Phys.* 9:899–907

Campus P, Christie DR. 2010. Worldwide observations of infrasonic waves. See Le Pichon et al. 2010, pp. 185–234

Chrzanowski P, Greene G, Lemmon KT, Young JM. 1961. Traveling pressure waves associated with geomagnetic activity. *J. Geophys. Res.* 66(11):3727–33

Chunchuzov IP. 2004. Influence of internal gravity waves on sound propagation in the lower atmosphere. *Meteorol. Atmos. Phys.* 85(1):61–76

Cook RK, Bedard AJ. 1971. On the measurement of infrasound. *Geophys. J. R. Astron. Soc.* 26:5–11

Courtier P, Andersson E, Heckley W, Pailleux J, Vasiljevic D, et al. 1998. The ECMWF implementation of three-dimensional variational assimilation (3D-Var). I: Formulation. *Q. J. R. Meteorol. Soc.* 124:1783–807

Daniels FB. 1952. Acoustical energy generated by the ocean waves. *J. Acoust. Soc. Am.* 24:83

Daniels FB. 1959. Noise-reducing line microphone for frequencies below 1 c/s. *J. Acoust. Soc. Am.* 31:529–31

de Groot-Hedlin CD. 2008. Finite-difference synthesis of infrasound propagation through an absorbing atmosphere. *J. Acoust. Soc. Am.* 124:1430–41

de Groot-Hedlin CD, Hedlin MAH, Drob DP. 2010. Atmospheric variability and infrasound monitoring. See Le Pichon et al. 2010, pp. 475–507

de Groot-Hedlin CD, Hedlin MAH, Walker K. 2011. Finite difference synthesis of infrasound propagation through a windy, viscous atmosphere: application to a bolide explosion detected by seismic networks. *Geophys. J. Int.* 185:305–20

de Groot-Hedlin CD, Hedlin MAH, Walker K, Drob D, Zumberge M. 2008. Study of propagation from the shuttle Atlantis using a large seismic network. *J. Acoust. Soc. Am.* 124(3):1442–51

de Larquier S, Pasko VP, Stenbaek-Nielsen HC, Wilson CR, Olson JV. 2010. Finite-difference time-domain modeling of infrasound from pulsating auroras and comparison with recent observations. *Geophys. Res. Lett.* 37:L06804

Donn WL, Rind D. 1971. Natural infrasound as an atmospheric probe. *Geophys. J. R. Astron. Soc.* 26:111–33

Drob DP, Garcés M, Hedlin MAH, Brachet N. 2010a. The temporal morphology of infrasound propagation. *Pure Appl. Geophys.* 167:437–53

Drob DP, Meier RR, Picone JM, Garcés MM. 2010b. Inversion of infrasound signals for passive atmospheric remote sensing. See Le Pichon et al. 2010, pp. 701–32

Drob DP, Picone JM, Garcés M. 2003. Global morphology of infrasound propagation. *J. Geophys. Res.* 108:4680

Ejakov SG, Phillips S, Dain Y, Lueptow RM, Visser JH. 2003. Acoustic attenuation in gas mixtures with nitrogen: experimental data and calculations. *J. Acoust. Soc. Am.* 113:1871–79

Evers LG, Haak HW. 2010. The characteristics of infrasound, its propagation and some early history. See Le Pichon et al. 2010, pp. 3–27

Fee D, Garcés M. 2007. Infrasonic tremor in the diffraction zone. *Geophys. Res. Lett.* 34:L16826

Fritts DC, Alexander MJ. 2003. Gravity wave dynamics and effects in the middle atmosphere. *Rev. Geophys.* 41:1003

Garcés M. 2004. On using ocean swells for continuous infrasonic measurements of winds and temperature in the lower, middle, and upper atmosphere. *Geophys. Res. Lett.* 31:L19304

Garcés M, Fee D, Steffke A, McCormack D, Servranckx R, et al. 2008. Capturing the acoustic fingerprint of stratospheric ash injection. *Eos Trans. AGU* 89:377–78

Garcés M, Hansen RA. 1998. Waveform analysis of seismoacoustic signals radiated during the fall 1996 eruption of Pavlof Volcano, Alaska. *Geophys. Res. Lett.* 25(7):1051–54

Garcés M, Hansen RA, Lindquist KG. 1998. Traveltimes for infrasonic waves propagating in a stratified atmosphere. *Geophys. J. Int.* 135:255–63

Garcés M, McNutt SR. 1997. Theory of the sound field generated by a resonant magma conduit. *J. Volcanol. Geotherm Res.* 78:155–78

Georges TM, Beasley WH. 1977. Refraction of infrasound by upper-atmospheric winds. *J. Acoust. Soc. Am.* 61(1):28–34

Gibson R, Drob D, Broutman D, Winslow N. 2010. Advancement of techniques for modeling the effects of atmospheric gravity-wave-induced inhomogeneities on infrasound propagation. *Proc. 2010 Monit. Res. Rev., Orlando, Fla., Sept. 21–23*, pp. 699–707. Washington, DC: Natl. Nucl. Secur. Adm.

Green DN, Vergoz J, Gibson R, Le Pichon A, Ceranna L. 2011. Infrasound radiated by the Gerdec and Chelopechene explosions: propagation along unexpected paths. *Geophys. J. Int.* 185:890–910

Gutenberg B. 1939. The velocity of sound waves and the temperature in the stratosphere in southern California. *Bull. Seismol. Soc. Am.* 20:192–201

Gutenberg B. 1958. Two types of microseisms. *J. Geophys. Res.* 63(3):595–97

Gutenberg B, Benioff H. 1941. Atmospheric-pressure waves near Pasadena. *Trans. Am. Geophys. Union* 22:424–26

Haubrich RA, McCamy K. 1969. Microseisms: coastal and pelagic sources. *Rev. Geophys.* 7:539–71

Hedlin MAH, Alcoverro B. 2005. The use of impedance matching capillaries for reducing resonance in rosette spatial filters. *J. Acoust. Soc. Am.* 117:1880–88

Hedlin MAH, Alcoverro B, D'Spain G. 2003. Evaluation of rosette infrasonic noise-reducing spatial filters. *J. Acoust. Soc. Am.* 114:1807–20

Hedlin MAH, Drob D, Walker K, de Groot-Hedlin CD. 2010. A study of acoustic propagation from a large bolide in the atmosphere with a dense seismic network. *J. Geophys. Res.* 115:B11312

Hedlin MAH, Raspet R. 2003. Infrasonic wind noise reduction by barriers and spatial filters. *J. Acoust. Soc. Am.* 114:1379–86

Hetzer CH, Waxler R, Gilbert KE, Talmadge CL, Bass HE. 2008. Infrasound from hurricanes: dependence on the ambient ocean surface wave field. *Geophys. Res. Lett.* 35:L14609

Holton JR. 1992. *An Introduction to Dynamical Meteorology*. San Diego, CA: Academic

Hornikx M, Waxler R, Forssen J. 2010. The extended Fourier pseudospectral time-domain method for atmospheric sound propagation. *J. Acoust. Soc. Am.* 128:1632–46

Ishihara Y, Tsukada S, Sakai S, Hiramatsu Y, Furumoto M. 2003. The 1998 Miyako fireball's trajectory determined from shock wave records of a dense seismic array. *Earth Planets Space* 55:e9–12

Johnson J, Aster RC, Ruiz MC, Malone SD, McChesney PJ, et al. 2003. Interpretation and utility of infrasonic records from erupting volcanoes. *J. Volcanol. Geotherm. Res.* 121:15–63

Jones RM, Riley JP, Georges TM. 1986. HARPA: a versatile three-dimensional Hamiltonian ray-tracing program for acoustic waves in an atmosphere above irregular terrain. *NOAA Rep.*, Environ. Res. Lab., Boulder, CO. 410 pp.

Kalnay M, Kanamitsu, Baker WE. 1990. Global numerical weather prediction at the National Meteorological Center. *Bull. Am. Meteorol. Soc.* 71:1410–28

Kanamori H, Mori J, Anderson DL, Heaton TH. 1991. Seismic excitation by the space shuttle Columbia. *Nature* 349:781–82

Kulichkov SN, Avilov KV, Popov OE, Otrezov AI, Bush GA, Baryshnikov AK. 2004. Some results of simulation of long-range infrasonic propagation in the atmosphere. *Izv. Atmos. Ocean. Phys.* 40:202–15

Kulichkov SN, Chunchuzov IP, Popov OI. 2010. Simulating the influence of an atmospheric fine inhomogeneous structure on long-range propagation of pulsed acoustic signals. *Izv. Atmos. Ocean. Phys.* 46:60–68

Langston C. 2004. Seismic ground motions from a bolide shock wave. *Geophys. Res. Lett.* 109:B12309

Le Pichon A, Blanc E, Drob D. 2005. Probing high-altitude winds using infrasound. *J. Geophys. Res.* 110:D20104

Le Pichon A, Blanc E, Hauchecorne A, eds. 2010. *Infrasound Monitoring for Atmospheric Studies*. Dordrecht: Springer. 735 pp. 1st ed.

Le Pichon A, Ceranna L, Garces M, Drob D, Millet C. 2006a. On using infrasound from interacting ocean swells for global continuous measurements of winds and temperature in the stratosphere. *J. Geophys. Res.* 111:D11106

Le Pichon A, Garcés M, Blanc E, Barthelemy M, Drob D. 2002. Acoustic propagation and atmosphere characteristics derived from infrasonic waves generated by the Concorde. *J. Acoust. Soc. Am.* 111:629–41

Le Pichon A, Guilbert J, Vallée M, Dessa JX, Ulziibat M. 2003. Infrasonic imaging of the Kunlun Mountains for the great 2001 China earthquake. *Geophys. Res. Lett.* 30:1814

Le Pichon A, Mialle P, Guilbert J, Vergoz J. 2006b. Multistation infrasonic observations of the Chilean earthquake of 2005 June 13. *Geophys. J. Int.* 167:838–44

Le Pichon A, Vergoz J, Blanc E, Guilbert J, Ceranna L, et al. 2009. Assessing the performance of the International Monitoring System's infrasound network: geographical coverage and temporal variabilities. *J. Geophys. Res.* 114:D08112

Lingevitch JF, Collins MD, Dacol DK, Drob DP, Rogers JC, Seigmann WL. 2002. A high angle and high Mach number parabolic equation. *J. Acoust. Soc. Am.* 111:729–34

Liszka L. 2008. Infrasound: a summary of 35 years of infrasound research. *IRF Sci. Rep. 291*, Swed. Inst. Space Phys. (Institutet för rymdfysik), Kiruna, Swed.

Longuet-Higgins MS. 1950. A theory of the origin of microseisms. *Philos. Trans. R. Soc. A* 243:1–35

Maeda K, Watanabe T. 1964. Pulsating aurorae and infrasonic waves in the polar atmosphere. *J. Atmos. Sci.* 21(1):15–29

Marston T, Gabrielson T. 2008. Modeling real porous tube infrasonic arrays. *J. Acoust. Soc. Am.* 123:3839
Matoza RS, Fee D, Garcés MA, Seiner JM, Ramon PA, Hedlin MAH. 2009. Infrasonic jet noise from volcanic eruptions. *Geophys. Res. Lett.* 36:L08303
Matoza RS, Garcés MA, Chouet BA, D'Auria L, Hedlin MAH, et al. 2008. The source of infrasound associated with long-period events at Mount St. Helens. *J. Geophys. Res.* 114:B04305
Matoza RS, Hedlin MAH, Garcés MA. 2007. An infrasound array study of Mount St. Helens. *J. Volcanol. Geotherm. Res.* 160(3–4):249–62
McDonald JA, Douze EJ, Herrin E. 1971. The structure of atmospheric turbulence and its application to the design of pipe arrays. *Geophys. J. R. Astron. Soc.* 26:99–109
Mikumo T. 1968. Atmospheric pressure waves and tectonic deformation associated with the Alaskan earthquake of March 28, 1964. *J. Geophys. Res.* 73:2009–25
Millet C, Robinet JC, Roblin C. 2007. On using computational aeroacoustics for long-range propagation of infrasounds in realistic atmospheres. *Geophys. Res. Lett.* 34:L14814
Mutschlecner JP, Whitaker RW. 2005. Infrasound from earthquakes. *J. Geophys. Res.* 110:D01108
Norris D, Gibson R, Bongiovanni K. 2010. Numerical methods to model infrasonic propagation through realistic specifications of the atmosphere. See Le Pichon et al. 2010, pp. 541–73
Olson JV, Wilson CR, Hansen R. 2003. Infrasound associated with the 2002 Denali fault earthquake, Alaska. *Geophys. Res. Lett.* 30:2195
Ostashev VE, Wilson DK, Liu L, Aldridge DF, Symons NP, Marlin D. 2005. Equations for finite-difference, time-domain simulation of sound propagation in moving inhomogeneous media and numerical implementation. *J. Acoust. Soc. Am.* 117:503–17
Pierce AD. 1989. *Acoustics: An Introduction to its Physical Principles and Applications*. Woodbury, NY: Acoust. Soc. Am.
Raspet R, Webster J, Dillon K. 2006. Framework for wind noise studies. *J. Acoust. Soc. Am.* 199:834–43
Rayleigh JWS. 1945 (1896). *The Theory of Sound*, Vol. 2. Mineola, NY: Dover. 2nd ed.
ReVelle DO. 2010. Acoustic-gravity waves from impulsive sources in the atmosphere. See Le Pichon et al. 2010, pp. 305–59
Rind D. 1980. Microseisms at Palisades 3: microseisms and microbaroms. *J. Geophys. Res.* 85:4854–62
Ripepe M, Marchetti E. 2002. Array tracking of infrasonic sources at Stromboli volcano. *Geophys. Res. Lett.* 29:2076
Shields FD. 2005. Low-frequency wind noise correlation in microphone arrays. *J. Acoust. Soc. Am.* 117:3489–96
Stopa JE, Cheung KF, Garcés MA, Fee D. 2011. Source of microbaroms from tropical cyclone waves. *Geophys. Res. Lett.* 38:L05602
Sutherland LC, Bass HE. 2004. Atmospheric absorption in the atmosphere up to 160 km. *J. Acoust. Soc. Am.* 115:1012–32
Symons GJ, ed. 1888. *The Eruption of Krakatoa and Subsequent Phenomena*. London: Trübner. 494 pp.
Tabulevich VN. 1995. On recordings of global microseismic vibrations and observations of microseisms in shore zones of oceans. *Phys. Earth Planet. Inter.* 91:299–305
Wald DJ, Jaiswal KS, Marano KD, Bausch DB, Hearne MG. 2010. PAGER—rapid assessment of an earthquake's impact. *U.S. Geol. Surv. Fact Sheet 2010-3036*, U.S. Geol. Surv., Golden, CO
Walker KT, Hedlin MAH. 2010. A review of wind-noise reduction methodologies. See Le Pichon et al. 2010, pp. 141–82
Walker KT, Hedlin MAH, de Groot-Hedlin CD, Vergoz J, Le Pichon A, Drob D. 2010. Source location of the 19 February 2008 Oregon bolide using seismic networks and infrasound arrays. *J. Geophys. Res.* 115:B12329
Walker KT, Shelby R, Hedlin MAH, de Groot-Hedlin CD, Vernon FL. 2011. Western U.S. Infrasonic Catalog: illuminating infrasonic hotspots with the USArray. *J. Geophys. Res.* 116:B12305
Walker KT, Zumberge M, Hedlin MAH, Shearer P. 2008. Methods for determining infrasound phase velocity direction with an array of line sensors. *J. Acoust. Soc. Am.* 124:2090–99
Warner CD, McIntyre ME. 1996. On the propagation and dissipation of gravity wave spectra through a realistic middle atmosphere. *J. Atmos. Sci.* 53:3213–35
Waxler R, Gilbert KE. 2006. The radiation of atmospheric microbaroms by ocean waves. *J. Acoust. Soc. Am.* 119:2651–64

Whipple FJW. 1935. The propagation of sound to great distances. *Q. J. R. Meteorol. Soc.* 61:285–308

Willis M, Garcés MA, Hetzer C, Businger S. 2004. Infrasonic observations of open ocean swells in the Pacific: deciphering the song of the sea. *Geophys. Res. Lett.* 31:L19303

Wilson CR. 1975. Infrasonic wave generation by aurora. *J. Atmos. Terr. Phys.* 37:973–88

Wilson CR, Olson JV, Stenbaek-Nielsen HC. 2005. High trace-velocity infrasound from pulsating auroras at Fairbanks, Alaska. *Geophys. Res. Lett.* 32:L14810

Wochner MS, Atchley AA, Sparrow VW. 2005. Numerical simulation of finite amplitude wave propagation in air using a realistic atmospheric absorption model. *J. Acoust. Soc. Am.* 118:2891–98

Yu J, Raspet R, Webster J, Abbott JP. 2011. Wind noise measured at the ground surface. *J. Acoust. Soc. Am.* 129:622–32

Zumberge MA, Berger J, Hedlin MAH, Husmann E, Nooner S, et al. 2003. An optical fiber infrasound sensor: a new lower limit on atmospheric pressure noise between 1 and 10 Hz. *J. Acoust. Soc. Am.* 113:2474–79

Annual Review
of Earth and
Planetary Sciences
Volume 40, 2012

Contents

Indexes

Errata

An online log of corrections to *Annual Review of Earth and Planetary Sciences* articles may be found at http://earth.annualreviews.org